Chemistry–A European Journal
Research Article
doi.org/10.1002/chem.202300618
Chemistry Europe
European Chemical Societies Publishing
www.chemeurj.org

Redox Reporter - Ligand Competition to Support Signaling in the Cocaine-Binding Electrochemical Aptamer-Based Biosensor

Philippe Dauphin-Ducharme,*[a] Zachary R. Churcher,[b] Aron A. Shoara,[b] Erfan Rahbarimehr,[a] Sladjana Slavkovic,[b] Nicolas Fontaine,[a] Olivia Boisvert,[a] and Philip E. Johnson*[b]

Abstract: Electrochemical aptamer-based (E-AB) biosensors have demonstrated capabilities in monitoring molecules directly in undiluted complex matrices and in the body with the hopes of addressing personalized medicine challenges. This sensing platform relies on an electrode-bound, redox-reporter-modified aptamer. The electrochemical signal is thought to originate from the aptamer undergoing a binding-induced conformational change capable of moving the redox reporter closer to the electrode surface. While this is the generally accepted mechanism, it is notable that there is limited evidence demonstrating conformational change or distance-dependent change in electron transfer rates in E-AB sensors. In response, we investigate here the signal transduction of the well-studied cocaine-binding aptamer with different analytical methods and found that this sensor relies on a redox-reporter - ligand competition mechanism rather than a ligand-induced structure formation mechanism. Our results show that the covalently bound redox reporter, methylene blue, binds at or near the ligand binding site on the aptamer resulting in a folded conformation of the cocaine-binding aptamer. Addition of ligand then competes with the redox reporter for binding, altering its electron transfer rate. While we show this for the cocaine-binding aptamer, given the prevalence of methylene blue in E-AB sensors, a similar competition-based may occur in other systems.

Introduction

Introduced in 2005, aptamer-based electrochemical (E-AB) biosensors have become ubiquitous in the literature to a point where they are now presented in widely used introductory textbooks.[1,2] E-AB biosensors are comprised of a ligand-specific, redox-reporter-modified aptamer sequence anchored on a gold electrode using thiol chemistry.[3] Upon ligand recognition, the aptamer is thought to undergo a binding-induced conformational change that alters the relative distance of the redox reporter with respect to the electrode surface.[3,4] This change alters the electron transfer rate of the redox reporter which can easily be measured using various electrochemical techniques to quantitatively report on the concentration of different molecules (i.e., antibiotics, chemotherapeutics, amino acids, drugs of abuse, etc.).[5] Given the scope of measurable ligands, E-AB sensors have been proposed to be generalizable thanks to the ease with which one aptamer recognition element can be swapped by another.[5] The electrochemical signal transduction scheme of E-AB sensors enables the direct deployment in undiluted whole blood and in the body,[6] which thus offers unprecedented and convenient measurement capabilities to transform our understanding of pharmacology and serve as personalized medicine tools.

While the conformational change mechanism for E-AB sensors has been postulated to be generalizable to several aptamers, little direct evidence is known about it. To start, evidence of aptamers used for E-AB sensing capable of undergoing conformational switching remain variable. To date, half of the studies have looked at aptamers using circular dichroism (CD)[6b,7] but this technique can only inform on a general structural change that is not necessarily the same as the one proposed for signal transduction in E-AB sensors. To circumvent this, others have attached a fluorophore/quencher pair to monitor conformational change in an aptamer.[8] However, modification has been shown to result in aptamer stabilization on the order of an additional base pair (~4 kJ mol^{-1})[9] which alters the conformational equilibrium it is designed to monitor. Other studies have looked at the cocaine-binding,[10] adenosine triphosphate-binding[11] and ampicillin-binding[12] aptamers using nuclear magnetic resonance (NMR) spectroscopy. While

[a] Dr. P. Dauphin-Ducharme, E. Rahbarimehr, Dr. N. Fontaine, O. Boisvert
Département de chimie
Université de Sherbrooke
Sherbrooke, QC J1K 2R1 (Canada)
E-mail: philippe.dauphin.ducharme@usherbrooke.ca

[b] Dr. Z. R. Churcher, Dr. A. A. Shoara, Dr. S. Slavkovic, Dr. P. E. Johnson
Chemistry Department
York University
4700 Keele Street, Toronto, Ontario M3J 1P3 (Canada)
E-mail: pjohnson@yorku.ca

Supporting information for this article is available on the WWW under https://doi.org/10.1002/chem.202300618

informative about the structural changes incurred by aptamers, these NMR studies have not used modified DNA sequences thus not offering a complete understanding of the changes incurred by the redox reporter and its ability to transduce a conformational rearrangement. Although these approaches are close solution equivalents to what happens on a surface, it remains unclear how target binding to aptamers in E-AB sensors can be transduced electrochemically.

The signaling mechanism of E-AB sensors is thought to rely on a distance-dependent change in the electron transfer of a redox reporter induced by a change in the conformation of the aptamer.[3,7e] To our knowledge, evidence of the generalizability of this mechanism toward other redox reporters remains scarce. Aside from a few publications discussing the stability of other redox reporters when attached to DNA,[13] the use of anthraquinone or exTTF to calibrate and correct E-AB sensor's drift,[14] a pH-independent osmium complex,[15] methylene blue remains the redox reporter of choice.[5] The widespread use of methylene blue stems from a redox potential that is conveniently positioned in a potential window devoid of other parasitic electrochemical processes (i.e., oxygen reduction and gold oxidation) on gold electrodes coated with an alkanethiol self-assembled monolayer. Though undergoing a complex proton-coupled electron transfer mechanism,[16] methylene blue strikingly shows, in contrast to other well-known outer-sphere redox reporters like ferrocene, reversible and stable electrochemical behavior when attached to DNA.[13] E-AB sensors relying on methylene blue, however, show dissociation constants several order of magnitudes greater than values determined using solution-based techniques (i.e., isothermal titration calorimetry (ITC), fluorescence, etc.)[11b,17] further raising questions to its implications in the signaling mechanism.

Here, we use a combinatorial approach of biophysical methods (i.e., ITC, NMR, fluorescence spectroscopy and electrochemistry) to investigate the structure and binding of the well-studied cocaine-binding aptamer in the presence of methylene blue either free or when covalently bound to mimic when adapted in its corresponding E-AB sensor. In doing so, we reveal an alternate mechanism through which signal is generated when methylene blue competes with the ligand at the ligand-binding site in the aptamer. We envision that unearthing this mechanism will prove useful in improving our understanding of E-AB sensors and facilitate a more rational approach in aptamer design and improve their translatability for biomedical use.

Results and Discussion

Assuming that signaling in E-AB sensors is driven by a distance-dependent change induced by the conformational state of an aptamer (Figure 1A), signaling should be independent of the redox reporter used. To investigate this, we decided to modify the termini of the well-characterized, structure-switching cocaine-and-quinine binding aptamer initially reported by Stojanovic[18] and further modified by Neves[10] into the MN19 variant with methylene blue or ferrocene. We then attached these aptamers onto gold electrodes using thiol chemistry and determined, using square-wave voltammetry and Lovric's formalism,[19] methylene blue and ferrocene electron transfer rates in the absence and presence of saturating amounts of quinine to determine the optimal square-wave frequencies for interrogation. Given its slower electrochemical reaction, we observed that differences in methylene blue transferred charge were maximized at a square-wave frequency <300 Hz (Figure S1A). Ferrocene, in contrast, required a square-wave

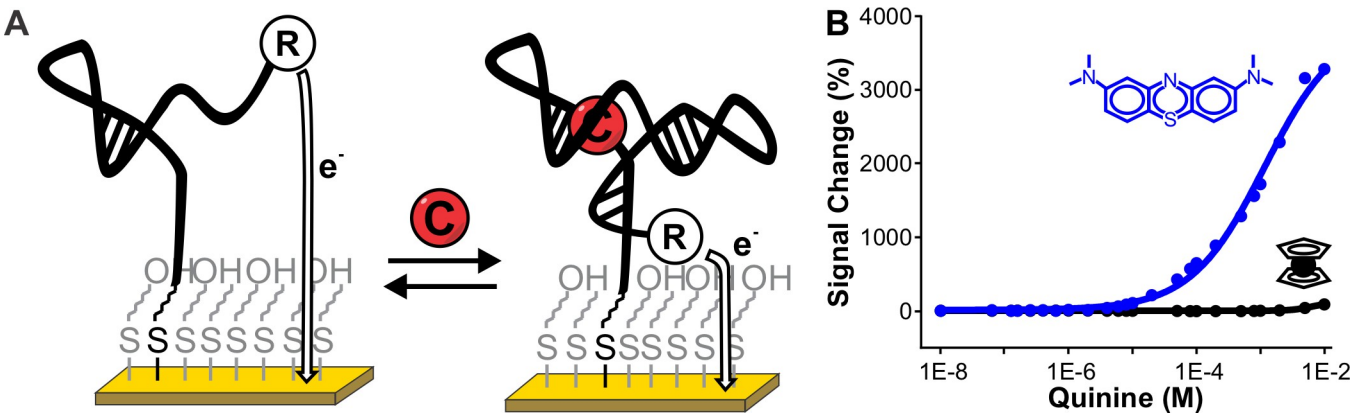

Figure 1. A) E-AB sensors are comprised of a redox-reporter-modified aptamer sequence attached on a gold electrode surface functionalized with a self-assembled monolayer, typically made of 6-mercaptohexanol. Signaling in this class of sensors is said to rely on a binding-induced change in electron transfer rates of the attached redox reporter induced by the aptamer's conformational change which displaces the redox reporter in closer vicinity to the electrode surface.[3] This can be easily monitored using square-wave voltammetry. Considering the proposed generalizability of the signaling mechanism to several aptamers, any redox reporter covalently attached to the aptamer should produce a measurable response with the proposed signaling mechanism. B) We investigated this with the cocaine-and-quinine binding aptamer's variant, MN19,[10] when modified with methylene blue (blue) or ferrocene (black). In doing so, we observed that the methylene blue-modified MN19 aptamer produced a maximal signal change of ~3200% when challenged with increasing amounts of quinine with a K_D value of 2 mM. The ferrocene-modified MN19 aptamer, in contrast, only produced ~130% at higher quinine concentrations (>5 mM). These results highlight the necessity of methylene blue for signaling in the quinine-and-cocaine E-AB sensor especially at the lower concentrations and suggest for an alternate mechanism that does not solely involve a distance-dependent change of the redox reporter.

frequency of >500 Hz to produce a discernable square-wave voltammogram peak (Figure S1B). Having identified the optimized square-wave frequency, we then interrogated both modified aptamers over an increasing amount of quinine and observed signal change of ~3200% in the case of the methylene blue modified aptamer in contrast to 132% for the ferrocene-modified aptamer (Figure 1B). While the ferrocene-modified aptamer did respond to quinine additions, it only did at high concentrations (>5 mM), values far exceeding the range at which this molecule should be detected[20] as opposed to the methylene-blue modified aptamer (>10 μM). Similar to the cocaine-and-quinine binding aptamer, we found that this observation also held when looking at an aptamer binding vancomycin when modified with methylene blue or ferrocene (Figure S1C). We thus concluded that, in contrast to ferrocene, methylene blue modification appeared essential to support strong E-AB signaling at low ligand concentrations and that the response produced had more to do with its molecular attributes.

We hypothesize that to produce such a high E-AB sensor response at low ligand concentrations, methylene blue, in contrast to ferrocene, may bind the aptamer and then be displaced by the ligand. The nucleic acid-binding property of methylene blue is well documented and has been reported to favorably occur with micromolar affinities via intercalation with GC-rich portions of DNA duplexes located in minor and major grooves.[21] This attribute has, for example, been utilized by Biniuri and co-workers to develop a fluorescent ATP switch aptamer-based sensor that is dependent on the oxidation state of methylene blue.[22] To support that this held with the MN19 aptamer, we performed ITC and fluorescence spectroscopy experiments to detect binding with methylene blue. ITC revealed at least two exothermic binding events (Figure 2A). While we were not able to accurately fit the data to either an independent or cooperative multisite binding model as we did previously with the ATP-binding DNA aptamer[11b] or the MN19 aptamer in low NaCl concentration,[23] we envision that these binding events could originate from two methylene blue molecules interacting with MN19. We confirmed via a control experiment of methylene blue titrated into a fixed concentration of methylene blue that dimerization of methylene blue molecules at concentrations past saturation of the aptamer was negligeable as we observe no binding signal for methylene blue binding methylene blue (Figure S2). We confirmed, using fluorescence spectroscopy, that methylene blue binds to the MN19 aptamer by using its emission properties. For this, we illuminated a methylene blue solution at 620 nm and monitored its emission at 683 nm while increasing the concentration of the MN19 aptamer. We observed that methylene blue fluorescence is quenched when in presence of the aptamer with an apparent K_D value of (7±2) μM. (Figure 2B). As previously discussed by Vardevanyan and co-workers,[24] this is in part associated to a change in the methylene blue environment resulting from intercalation. While we cannot account for methylene blue binding to a single or to two distinct sites on the MN19 aptamer, methylene blue fluorescence is altered due to its interaction with this aptamer. Together, both the fluorescence and ITC results support our proposal that methylene blue binds to the MN19 cocaine-and-quinine binding aptamer.

The binding of methylene blue folds the MN19 cocaine-and-quinine binding aptamer. We observed this in solution when monitoring imino ^{1}H signals in the NMR spectrum of MN19 while increasing methylene blue concentration (Figure 3A). As previously reported, the NMR spectrum of unbound MN19 is missing a number of resonances expected if the aptamer was

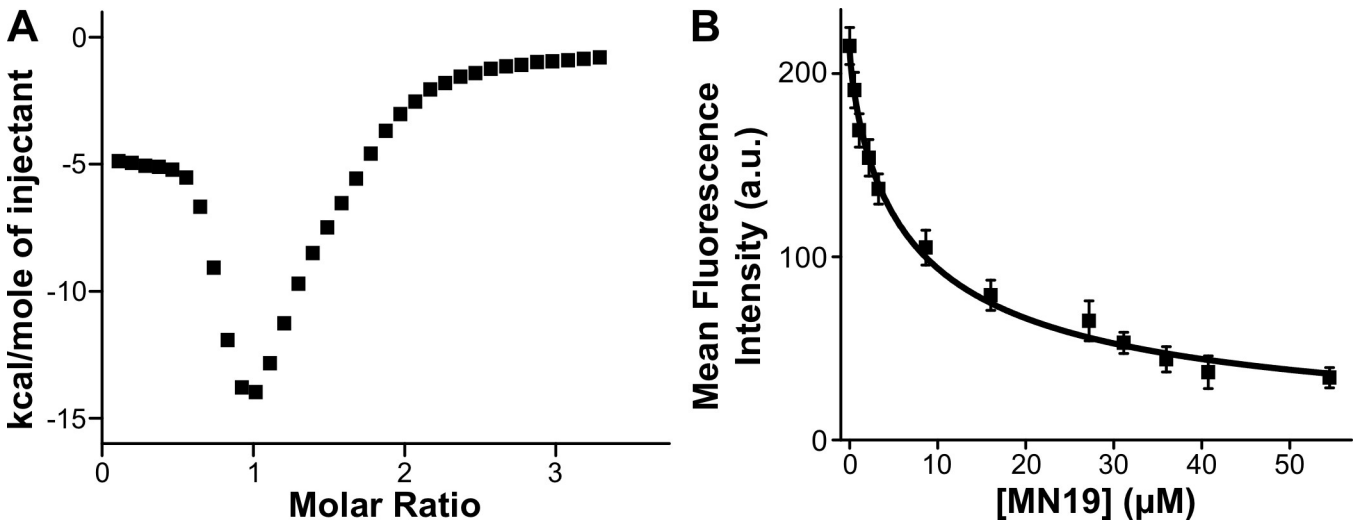

Figure 2. Methylene blue binds to the MN19 cocaine-and-quinine binding aptamer. A) We observed this using ITC methods when we titrated a fixed concentration of the MN19 aptamer with increasing amounts of methylene blue. In doing so, we observed multiple exothermic binding events that originate from methylene blue binding to the MN19 aptamer (see additional control in Figure S2). B) We further confirmed this using methylene blue fluorescence. In exciting a solution of methylene blue at 620 nm when at a fixed concentration while measuring its relative mean fluorescence intensity at 683 nm as a function of increasing amounts of the MN19 aptamer, we observed a drop in the fluorescence intensity. We thus concluded from our ITC and fluorescence results that methylene blue binds the MN19 aptamer.

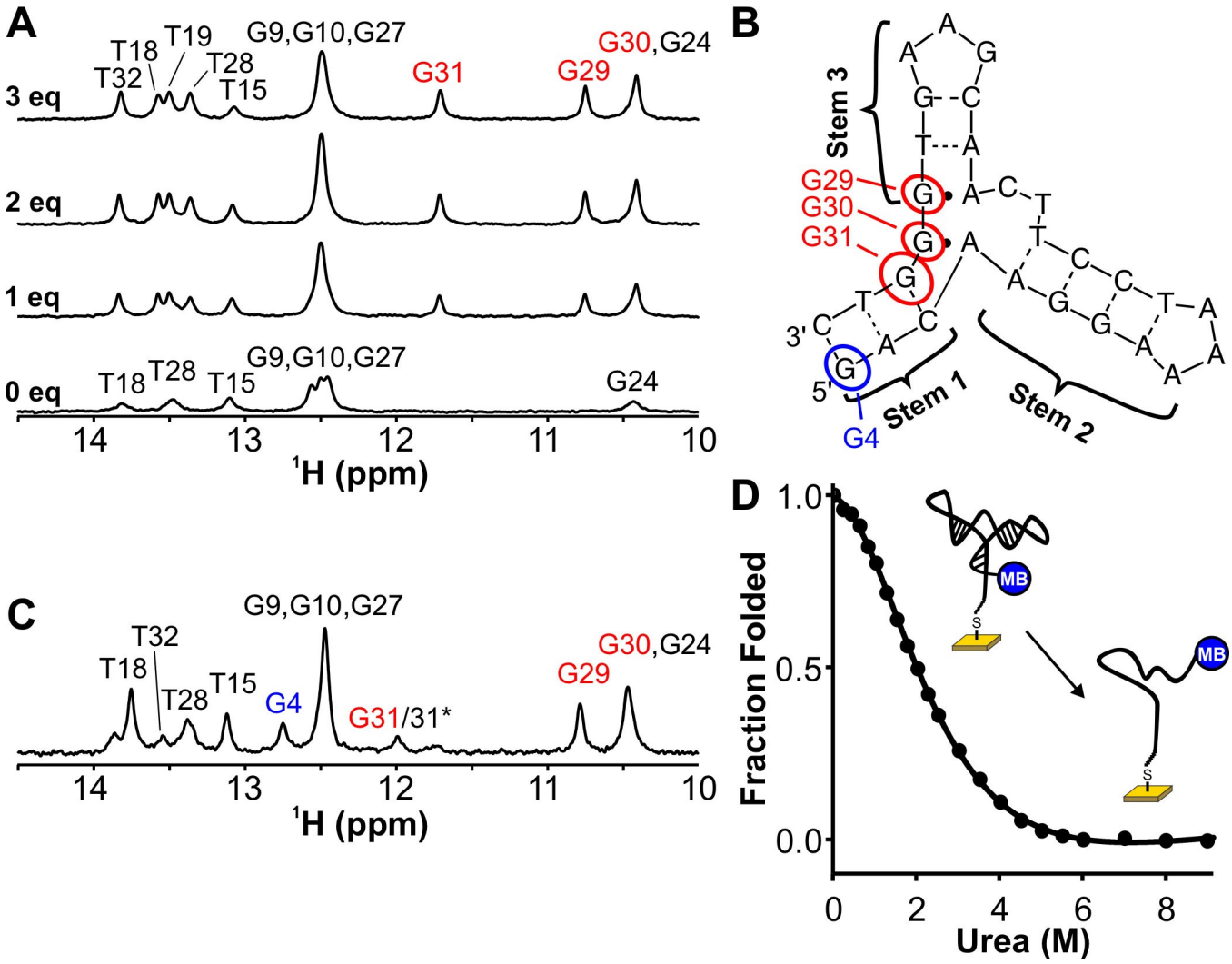

Figure 3. The binding of methylene blue folds the MN19 cocaine-and-quinine binding aptamer. A) We determined this by titrating the MN19 aptamer with increasing amounts of methylene blue and recorded its 1D ^{1}H NMR spectrum. In the free state, MN19 shows the spectrum of a partially folded, or dynamic molecule. Upon addition of methylene blue, binding occurs and the full complement of imino ^{1}H signals appear. B) The appearance of imino ^{1}H signals is particularly noticeable for G29, G30 and G31 (see Figure S3 for assignment). We did not observe these signals prior to addition of methylene blue. We presume that this is because, in absence of methylene blue, the MN19 aptamer is in a partially unstructured form and that those guanines are not involved or only weakly involved in base pairing. C) Covalent modification of the MN19 at the 3′ extremity with methylene blue also folds its structure. We observed this when looking at the imino ^{1}H peak of G4, G29, G30 and G31. The presence of all peaks indicates base pairing that we envisioned can only form upon the MN19 aptamer folding and forming stem 1. D) Methylene blue-induced aptamer folding holds when attached on electrodes. We observed this when performing an electrochemical urea denaturation curve of the surface-attached, methylene-blue-modified MN19 aptamer. Our results show that more than 98% of surface-attached MN19 aptamers are folded and that more than 4 M of urea is required to fully unfold its structure.

fully folded.[10,25] As methylene blue is added, the imino proton peaks, initially very broad or not visible, sharpen (Figure 3A). This process is indicative of ligand-induced folding of the MN19 aptamer upon methylene blue binding where the most notable resonances to appear are those of G29, G30 and G31 (see resonance assignment with 2D NOESY in Figure S3). These nucleotides lie in stem 1 and at the three-way junction of the aptamer which, according to our previous reports, appear only in the ligand-bound (cocaine, quinine, quinine-based antimalarial compounds or hemicyanine-based dyes) NMR spectra of the MN19 aptamer.[10,17b,25a,26]

Covalent attachment of methylene blue also folds the MN19 cocaine-and-quinine binding aptamer when in solution. We investigated this in solution by looking at the imino ^{1}H signals in the NMR spectrum of the 3′-modified methylene blue MN19, the same modification typically used in E-AB sensors (Figure 3C). In doing so, we measured sharper signals than what we initially measured when no methylene blue is present (Figure 3A) and observed distinct peaks of G4, G29, G30 and G31 (Figure 3B and C). We presume that the addition of methylene blue leads to the presence of the G4 signal due to a reduction in the stems breathing motions and thus the disappearance of the signals associated with the terminal base pairs. This indicates that the covalently attached methylene blue induces the folding of the MN19 aptamer to that of its ligand-bound state.

We confirmed that folding induced by the covalent attachment of methylene blue also holds when the aptamer is attached to electrodes. For this, we performed a denaturation experiment in which we subject MN19 E-AB sensors to increasing amounts of the chemical denaturant urea.[27] By monitoring the methylene blue peak current in square-wave voltammetry of the MN19-modified gold electrodes, we observed a decrease in peak current that we attribute to the unfolding of the aptamer. Such a decrease in peak current required more than 4 M of urea to fully unfold the aptamers and thus we found that more than 98% of aptamers attached on electrodes were initially in their folded forms (Figure 3D). Together, both solution and surface measurements indicate that in addition to binding to the MN19 aptamer, methylene blue appears to stabilize its structure and act as an additional ligand through which the MN19 cocaine-and-quinine binding aptamer undergoes folding.

Cocaine competes with methylene blue for binding to the MN19 aptamer. We investigated this by titrating fixed molar equivalents of cocaine into the methylene blue-bound MN19 aptamer complex using fluorescence, ITC and NMR spectroscopy. Our fluorescence results revealed that the emission, initially quenched due to methylene blue binding to the aptamer, is in part restored as we increased the cocaine concentration (Figure 4A). Our ITC results of the same system also show displacement of methylene blue as cocaine is added since we measure a single exothermic event that we attribute to the displacement of methylene blue by cocaine (Figure 4B). We hypothesize that these observations are a result of cocaine competing with methylene blue to bind a common site on the aptamer. Given the K_D value of methylene blue to the MN19 aptamer (from fluorescence of (7 ± 2) μM) and cocaine to MN19 (26 μM),[10] we envision that ligand binding to MN19 occurs competitively with methylene blue. We observed this competitive behavior between ligand and methylene blue when looking at the imino ^{1}H NMR spectrum. Addition of cocaine to the methylene blue-MN19 complex, for example, revealed that imino ^{1}H-associated peaks initially sharp, become broadened as cocaine is added and the aptamer is in exchange between the methylene blue- and cocaine-bound states, with no single state predominating (Figure 4C). Indicative of this, we observe that the resonance of G31 in MN19 was initially sharp then separated into two broad peaks, one for each of the two complexes. This indicates the formation of two states that coexist due to the similarity of methylene blue and cocaine K_D values. Given the proximity of G31 to the ligand binding site of MN19, we think that both methylene blue and cocaine compete for the same aptamer binding site. In support of this competition model, we note that the SS1 DNA sequence that we have previously used as a negative control for cocaine and quinine binding to the cocaine-binding aptamer,[28] due to a mutation in the ligand binding site, does not bind methylene blue (Figure S4). This indicates that both methylene blue and MN19's ligands cocaine and quinine share a common binding site.

Covalently attached methylene blue also competes with cocaine for binding in the MN19 aptamer. We investigated this with the MN19 aptamer modified at its 3′ end with methylene blue using fluorescence, ITC and NMR spectroscopy. In agreement with our observations for the free in solution methylene blue (Figure 4A), our fluorescence results showed that when covalently modified methylene blue MN19 is challenged with increasing amounts of cocaine, emission increased (Figure 5A) following a Langmuir-Hill type behavior with an apparent K_D value of 3.64 μM. This apparent affinity constant is tighter than for the unconjugated methylene blue displacement by cocaine (i.e., 7 ± 2 μM as shown in Figure 4A). We attributed the increase in fluorescence to methylene blue being displaced from the MN19 aptamer which changes its environment and its emission properties.[24] ITC experiments also showed that the

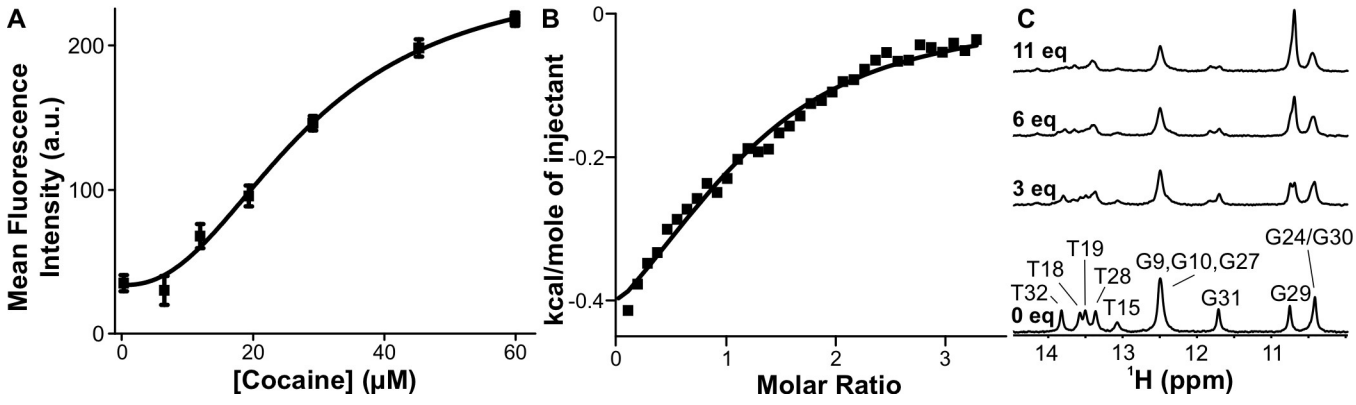

Figure 4. Cocaine competes with methylene blue binding in the MN19 cocaine-and-quinine binding aptamer. A) We measured this by exposing the methylene blue MN19 complex to increasing amounts of cocaine. The fluorescence of methylene blue, initially quenched as it is bound to the aptamer, started to increase, indicative of displacement. B) We likewise observed methylene blue displacement from the aptamer when subjecting the methylene blue-MN19 complex with increasing amounts of cocaine in ITC. Doing so resulted in a single exothermic event. While smaller than what we observed for methylene blue binding to the aptamer in Figure 2(A), we envision that this is due to simultaneous competitive binding of cocaine and methylene blue to the aptamer. (**C**) NMR spectroscopy confirmed this ligand-methylene blue competition when looking at the imino ^{1}H peaks of the methylene blue-MN19 complex. Peaks, initially sharp, started to broaden as the concentration of cocaine increased. The peak associated with G31, located near the presumed ligand binding site of MN19 started to appear as two signals as we added increasing amounts of cocaine. We hypothesize that this is because both cocaine and methylene blue compete as ligands for the same binding site on the aptamer with the cocaine not fully displacing the methylene blue.

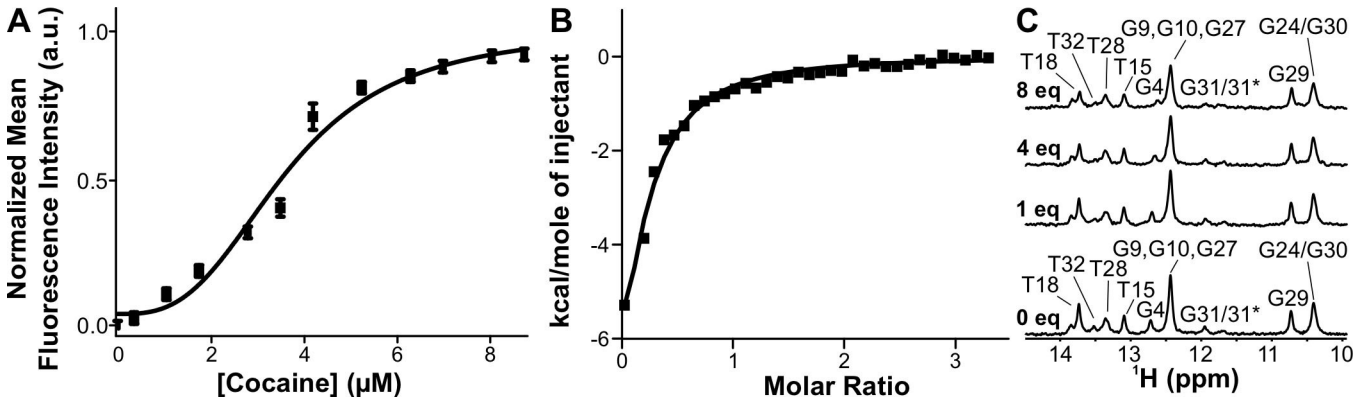

Figure 5. Redox reporter - ligand-competition still holds when methylene blue is covalently attached to the MN19 aptamer. A) We observed this when monitoring methylene blue fluorescence emission as a function of increasing amounts of cocaine to the methylene blue-labelled MN19 aptamer. In doing so, we measured an increase in methylene blue fluorescence because of its displacement from the aptamer following a Langmuir-Hill-type behavior with a K_D value of 3.64 μM. B) Our ITC results also support cocaine binding to the methylene blue-labelled MN19 aptamer. When titrating increasing amounts of cocaine to the conjugated aptamer, we measured an exothermic reaction that we associated with aptamer binding. C) NMR results support ligand competition with the methylene blue conjugated aptamer. Aside from a small upfield shift and a small broadening of peaks assigned to G4 and G31, respectively, as we increased cocaine concentrations, we do not observe significant changes in imino ^{1}H resonances. We hypothesize that this is because, as ligand concentration is increased, the MN19 aptamer maintains its structure and only competition between the two ligands binding at a common site is observed. D) Binding of the redox reporter to the aptamer also occurs competitively with ligands when attached onto electrodes. We observed this by looking at the relative E-AB sensor response's when challenged with chloroquine, quinine, primaquine and cocaine, which possess different aptamer affinity.[17b] We measured the largest decrease in normalized charge transfer resistance for chloroquine, the molecule that has the highest affinity for this class of aptamer.

methylene blue-conjugated aptamer still allowed for cocaine binding. When exposing the methylene blue-labelled aptamer to increasing amounts of cocaine using ITC, we measured an exothermic binding event (Figure 5B). We measure a more exothermic binding event when cocaine displaces the conjugated methylene blue than the bound methylene blue (Figure 5B vs. 4B) and a less exothermic binding event than previous measurements for the unlabeled MN19 aptamer.[29] We hypothesize that this likely arises as the conjugated methylene blue is more easily displaced due to intramolecular constraints (see above fluorescence results) and must bind in a less exothermic manner than the unconjugated methylene blue. When we investigated the methylene blue-conjugated aptamer using NMR, we observed that it still was subject to a competitive ligand binding mechanism. Aside from a small upfield shift and a broadening of peaks associated with G4 and G31, respectively, exposure of the MN19 aptamer to increasing amounts of cocaine, produced little discernable imino ^{1}H signatures changes (Figure 5C). This likely is because for the conjugated methylene blue aptamer, methylene blue is displaced more easily than the unconjugated methylene blue and the resulting complex in the NMR sample predominantly shows one species, resulting in less line broadening. Together our results support that methylene blue competes with ligand binding and that the structure of the aptamer remains folded only allowing for exchange between both the cocaine and methylene blue-bound states to occur.

Surface-attachment of methylene blue modified aptamers also reveal redox-reporter - ligand competition. We observed this when we investigated MN19 E-AB biosensors using electrochemical impedance spectroscopy with increasing amounts of cocaine. While applying a fixed sinusoidally oscillating potential centered around the methylene blue redox potential, we measured the phase shift of the AC current response from 10 kHz to 0.1 Hz (Figure S5). Upon addition of increasing amounts of cocaine, the phase peak initially centered <1 Hz started to incrementally shift toward higher interrogating frequencies. Such results support the formation of different electron transfer states at each ligand concentration. In contrast to the vastly accepted two-state model (Figure 1A), which would result in the formation of two distinct states (i.e., unbound and bound conformations) with peaks at fixed frequencies, instead we measure concentration-dependent phase peaks. This supports that the electron transfer rate of methylene blue changes following a Langmuir-Hill type model upon addition of ligand. We likewise observed that when titrating MN19 E-AB biosensors with different ligands (chloroquine, quinine, primaquine and cocaine) of varying affinities,[17b] that the maximal electrochemical response changed accordingly. In looking at the highest affinity ligand (chloroquine), we measured the largest decrease in the charge transfer resistance of the E-AB biosensor. We measured the lowest decrease in charge transfer, in contrast, for the ligand with the lowest affinity for MN19 (cocaine). We presume that those results indicate that ligands showcasing higher affinities for the aptamer compete with methylene blue allowing for an increased displacement. We thus think that our electrochemical impedance spectroscopy results again support for a redox-reporter - ligand competition model.

Discussion

Given the results we obtained here with fluorescence spectroscopy, ITC, NMR, and electrochemistry, we propose an alternative signal transduction mechanism for the MN19 quinine-

and-cocaine E-AB sensor that we refer as "redox-reporter – ligand competition" (Figure 6). Our proposed mechanism, in contrast to the widely accepted "binding-induced conformational change" mechanism (Figure 1A), which implies that the aptamer follows a "two-state system" (i.e., unbound and bound), first involves methylene blue binding the MN19 aptamer resulting in aptamer folding. Our results indicate that the proximity of methylene blue with the ligand binding site supports E-AB sensor signaling because the redox reporter competes with ligand binding. Upon ligand binding, methylene blue is displaced which allows it to support optical and electrochemical signaling. While we present our proposed mechanism as an intramolecular binding event of methylene blue with the aptamer, we cannot dismiss the possibility that methylene blue binds with neighboring aptamers once on the electrode.[30] In resorting to methylene blue, we foresee that our proposed redox-reporter - ligand competition mechanism will limit the ability of the MN19 E-AB sensor to detect ligands that: 1) have affinities similar or tighter for the aptamer than the aptamer has for methylene blue; and 2) bind in the vicinity of methylene blue. Achieving both feats is essential to support signaling for the MN19 E-AB sensor. We presume that because methylene blue binds in the vicinity of the ligand binding site and folds the MN19 aptamer explains the large and unprecedented 3200% signal response of the sensor we measured for quinine in contrast to the ferrocene-modified aptamer, a molecule that does not possess the same aptamer-binding attributes.

We think that with our proposed redox-reporter - ligand competition mechanism and the broad analytical methodology used here provides alternatives to improve the design of aptamers and their use in electrochemical biosensors. To start, with a deeper understanding of the structure-function of other aptamers and the role of the redox reporter in signal transduction, we foresee that this can, in turn, improve the high attrition rate in the translation of aptamers into electrochemical biosensors.[5] For example, by identifying the DNA binding motifs for a redox reporter, it may be possible to insert that motif in the vicinity of the conserved regions (i.e., the binding motif found in multiple aptamer candidates following selection) of an aptamer to systematically create a redox reporter – ligand competition mechanism. Similarly, one can foresee that instead of directly attaching methylene blue at the 3'-end of the aptamer that this extremity could be further extended to enhance its flexibility and influence the ability of methylene blue to bind with the aptamer. While we studied a single aptamer here, we anticipate that our proposed mechanism could be broadly applicable to other aptamer systems given the prevalence of methylene blue in all reported E-AB sensors. One could, for instance, build on the large literature of redox intercalative dyes[31] and introduce other redox reporters that have DNA binding attributes to support E-AB signaling. Doing so would not only provide alternatives within the scanned potential window, it would also help tune the dynamic range of an E-AB sensor due to competition for the ligand binding site. Finally, given the implication of methylene blue in the MN19 E-AB sensor signal transduction, we propose that this should be taken into consideration when developing the systematic evolution of ligand by exponential enrichment (SELEX) schemes for aptamers intentionally tailored for E-AB sensing. Together, we foresee that these various principles will improve how aptamers should be designed to support E-AB sensor signaling and in turn help for their translation into "real-world" applications.

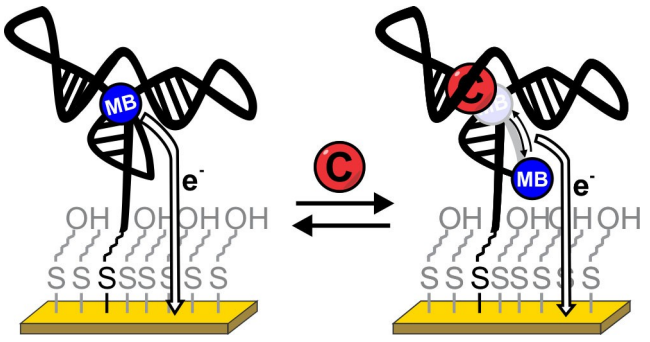

Figure 6. The ability of the redox reporter to bind in the vicinity of the ligand binding site of the MN19 aptamer is pivotal in generating signal change in the cocaine-and-quinine binding E-AB sensor. In this case, methylene blue binds in the vicinity of the cocaine and quinine ligand binding site, allowing for its structure to fold. The addition of ligand displaces the methylene blue from this site and alters either its proximity with the electrode or its environment ultimately changing its electron transfer rate. Our results thus show that instead of the broadly accepted mechanism through which aptamers undergo a binding-induced conformational change, signaling in the MN19 E-AB sensor is rather supported by a "redox reporter – ligand competition" mechanism.

Conclusions

We have explored the signal transduction mechanism of the cocaine-and-quinine E-AB sensor. In doing so, we have found that the commonly used redox reporter methylene blue in this class of sensors folds the cocaine-and-quinine binding MN19 aptamer and that it competes with ligand binding. As a result of this competition, methylene blue is displaced from the aptamer binding pocket and this change alters its fluorescence and electrochemical properties which are used to transduce ligand binding into a measurable signal. We thus propose that, in contrast to the widely accepted "conformational change", signal transduction by this E-AB sensor is supported by a "redox reporter – ligand competition" mechanism. In having this alternate mechanism in mind, new aptamer-design guidelines can be developed which we hope will help improve the translation of aptamers into the E-AB sensing platform to further expand the number of molecules these sensors can measure in complex matrices and in the body.

Experimental Section

Surface measurements: E-AB sensors were fabricated following an established protocol (see Supporting Information for more details).[32] We interrogated E-AB sensors with square-wave voltammetry using a 1 mV increment, 25 mV amplitude, the appropriate

frequency depending on the electron transfer rate determined for the redox reporter when in absence or presence of target (i.e., quinine hydrochloride or urea (Sigma Aldrich, Ontario, Canada)), and an adjusted potential window depending on the redox reporter (i.e., −0.1 to −0.5 V for methylene blue and 0 to 0.4 V for ferrocene). In doing so, we made sure sensors fabricated using each reporter were independently optimized. We then exposed E-AB sensors to increasing amounts of target and verified that addition did not influence the pH of our buffer. Given the limited solubility of quinine in buffer, we prepared the highest concentration stock of quinine at 20 mM using 2 mL of ethanol that we then diluted with 4 mL of 1X phosphate buffered saline (PBS) solution. Only the last point of our titration experiment surpassed 10% of ethanol in the electrochemical cell. For the chemical denaturation experiment, we prepared urea (Sigma Aldrich, Ontario, Canada) solution using 1X PBS at a stock concentration of 9.8 M which we then add in the electrochemical cell depending on the desired concentration. We interrogated sensors at a 5 Hz square-wave frequency while increasing the concentration of urea. We normalized the resulting measured peak current at each urea concentration prior to deriving fraction folded by subtracting the dependency of the electrochemical signal at high and low concentrations of urea as per past literature.[27b]

We interrogated E-AB sensors with electrochemical impedance spectroscopy via a potentiostatic measurement which consisted in varying a sinusoidally oscillating potential between 10 kHz and 0.1 Hz with a 10 mV amplitude while fixing the potential halfway between the oxidation and reduction waves of methylene blue as determined by a cyclic voltammogram acquired between 0 and −0.5 V vs Ag|AgCl. We degassed our electrochemical cell using a constant flow of Ar given the lower charge transfer rate of MN19. We repeated this measurement at each concentration of target (i.e., chloroquine, primaquine and cocaine, which we all acquired from Sigma Aldrich and prepared stocks of the molecules either directly in 1X PBS or in 100% DMSO that we then dilute to the desired concentrations in 1X PBS). We then perform a non-linear fit of our impedimetric trace using BioLogic algorithms to a previously reported equivalent circuit diagram[33] to determine the interfacial charge transfer resistance, a parameter inversely associated with the electron transfer reaction of the redox reporter. We then plotted these values as a function of target concentration which we fitted to a Langmuir-Hill equation K_D.

Isothermal titration calorimetry experiments: Isothermal titration calorimetry experiments were performed using a MicroCal VP-ITC instrument in a manner similar as described previously (see Supporting Information for more details).[34] All experiments were acquired at 15 °C and corrected for the heat of dilution of the titrant. Titrations were performed with a 60 μM aptamer sample in the cell and a 936 μM solution of the ligand, the titrant, in the needle.

The displacement ITC experiment was performed using a 1:1 molar solution of MN19 and methylene blue prepared with a concentration of 60 μM of each in 1X PBS and placed in the cell, while a 936 μM solution of cocaine in 1X PBS was prepared and placed in the syringe. Cocaine was titrated into the MN19 and methylene blue solution to measure the heat of cocaine displacing the bound methylene blue from the MN19 aptamer. All ITC binding experiments consisted of 35 successive 8 μL injections spaced every 300 s, where the first injection was 2 μL. When possible, data were fit to a one-site binding model using Origin 7 software.

Fluorescence spectroscopy experiments: Fluorescence experiments were carried out using a Cary Eclipse fluorescence spectrofluorometer in a manner as described previously.[35] We titrated the MN19 aptamer into 0.13 μM methylene blue dissolved in 1X PBS at 20 °C. We then excited methylene blue at 620 nm while we measured the steady-state fluorescence at an emission wavelength range of 630–800 nm in four 10-mm quartz cuvettes (where one is a blank PBS sample for a negative control). We incrementally increased the MN19 aptamer aliquots to 54.5 μM as methylene blue emission was recorded. Then, the obtained integrated emission intensities for each titration point were averaged and plotted as a function of methylene blue concentration. To quantify the apparent dissociation constant (K_D) and compare the interaction affinities, we fitted the obtained curves to a nonlinear binding function as described previously using OriginPro software package (OriginLab 2016, Northampton, USA).[29]

To displace methylene blue from the aptamer, we titrated cocaine into the bound methylene blue-MN19 complex sample. We then averaged the observed methylene blue emission results from four independent trials and plotted those as a function of cocaine concentration values. Since the studied aptamers and cocaine had no light absorbance at or beyond 620 nm, the inner-filter effect for the loss of excitation and emission light intensities was not calculated.

We studied the covalently-attached methylene blue MN19 aptamer (MB-MN19) by measuring the steady-state fluorescence emission of 0.1 μM of the conjugated aptamer prepared in 1X PBS to a final cocaine concentration of 8.7 μM in PBS at 20 °C. We excited methylene blue at 620 nm. Then, the obtained integrated emission intensities for each titration point from four independent trials were averaged and analyzed as a function of cocaine concentration as described above.

NMR spectroscopy experiments: We acquired ^{1}H NMR spectra of MN19 and covalently-labelled methylene blue MN19 in 140 mM NaCl, 10 mM $Na_xH_yPO_4$ at pH 6.8 in 10% ^2H_2O/90% ^1H_2O at 5 °C with concentrations of 160–500 μM DNA in a manner generally described previously.[36] We prepared a methylene blue stock solution by dissolving methylene blue in the above buffer. We first titrated methylene blue into MN19 to a final molar ratio of 3:1 methylene blue:MN19 aptamer. We then titrated cocaine into this sample to a final molar ratio of 11:1 cocaine:MN19 aptamer. We performed a two-dimensional ^{1}H-^{1}H NOESY experiment on methylene blue-bound MN19 with a mixing time (τ_m) of 200 ms. For the 2D experiment, we used an aptamer concentration of 1.2 mM with a molar ratio of aptamer:methylene blue of 1:2. For the competition experiment of covalently labelled methylene blue MN19 we used a concentration of 160 μM of the modified aptamer and added cocaine to a final molar ratio of 1:8 modified aptamer: cocaine. Water suppression for all experiments was achieved using excitation sculpting.

Acknowledgements

The authors thank Dr. Logan Donaldson (York University) for the use of the fluorescence spectrometer. The authors acknowledge the Natural Sciences and Engineering Research Council of Canada for funding this project via the Discovery Grant program. P.D.-D. would also like to acknowledge the Fonds de recherche Nature et Technologies for funding through the program: Établissement de la relève professorale and NOVA program.

Conflict of Interests

The authors declare no conflict of interest.

Data Availability Statement

The data that support the findings of this study are available from the corresponding author upon reasonable request.

Keywords: aptamer · electrochemical aptamer-based biosensors · methylene blue · NMR · isothermal calorimetry titration

[1] A. J. Bard, L. R. Faulkner, H. S. White, *Electrochemical Methods: Fundamentals and Applications*, John Wiley & Sons, **2022**, pp. 805–807.
[2] D. C. Harris, C. A. Lucy, *Quantitative Chemical Analysis*, W. H. Freeman, **2019**, p. 428.
[3] Y. Xiao, B. D. Piorek, K. W. Plaxco, A. J. Heeger, *J. Am. Chem. Soc.* **2005**, *127*, 17990–17991.
[4] B. R. Baker, R. Y. Lai, M. S. Wood, E. H. Doctor, A. J. Heeger, K. W. Plaxco, *J. Am. Chem. Soc.* **2006**, *128*, 3138–3139.
[5] N. Arroyo-Currás, P. Dauphin-Ducharme, K. Scida, J. L. Chávez, *Anal. Methods* **2020**, *12*, 1288–1310.
[6] a) N. Arroyo-Currás, J. Somerson, P. A. Vieira, K. L. Ploense, T. E. Kippin, K. W. Plaxco, *Proc. Natl. Acad. Sci. USA* **2017**, *114*, 645–650; b) P. Dauphin-Ducharme, K. Yang, N. Arroyo-Currás, K. L. Ploense, Y. Zhang, J. Gerson, M. Kurnik, T. E. Kippin, M. N. Stojanovic, K. W. Plaxco, *ACS Sens.* **2019**, *4*, 2832–2837; c) A. Idili, N. Arroyo-Currás, K. L. Ploense, A. T. Csordas, M. Kuwahara, T. E. Kippin, K. W. Plaxco, *Chem. Sci.* **2019**, *10*, 8164–8170.
[7] a) Y. Wu, S. Ranallo, E. Del Grosso, A. Chamoro-Garcia, H. L. Ennis, N. Milosavić, K. Yang, T. Kippin, F. Ricci, M. Stojanovic, K. W. Plaxco, *Bioconjugate Chem.* **2023**, *34*, 124–132; b) K. M. Cheung, K.-A. Yang, N. Nakatsuka, C. Zhao, M. Ye, M. E. Jung, H. Yang, P. S. Weiss, M. N. Stojanović, A. M. Andrews, *ACS Sens.* **2019**, *4*, 3308–3317; c) H. Fujita, Y. Imaizumi, Y. Kasahara, S. Kitadume, H. Ozaki, M. Kuwahara, N. Sugimoto, *Pharmaceuticals* **2013**, *6*, 1082–1093; d) A. A. Rowe, E. A. Miller, K. W. Plaxco, *Anal. Chem.* **2010**, *82*, 7090–7095; e) Y. Xiao, T. Uzawa, R. J. White, D. DeMartini, K. W. Plaxco, *Electroanalysis* **2009**, *21*, 1267–1271.
[8] a) M. N. Stojanovic, P. de Prada, D. W. Landry, *J. Am. Chem. Soc.* **2001**, *123*, 4928–4931; b) A. J. Simon, A. Vallée-Bélisle, F. Ricci, K. W. Plaxco, *Proc. Natl. Acad. Sci. USA* **2014**, *111*, 15048–15053.
[9] B. G. Moreira, Y. You, R. Owczarzy, *Biophys. Chem.* **2015**, *198*, 36–44.
[10] M. A. D. Neves, O. Reinstein, P. E. Johnson, *Biochemistry* **2010**, *49*, 8478–8487.
[11] a) C. H. Lin, D. J. Patei, *Chem. Biol.* **1997**, *4*, 817–832; b) S. Slavkovic, Y. Zhu, Z. R. Churcher, A. A. Shoara, A. E. Johnson, P. E. Johnson, *Sci. Rep.* **2020**, *10*, 18944.
[12] F. Bottari, E. Daems, A.-M. de Vries, P. Van Wielendaele, S. Trashin, R. Blust, F. Sobott, A. Madder, J. C. Martins, K. De Wael, *J. Am. Chem. Soc.* **2020**, *142*, 19622–19630.
[13] D. Kang, F. Ricci, R. J. White, K. W. Plaxco, *Anal. Chem.* **2016**, *88*, 10452–10458.
[14] a) H. Li, N. Arroyo-Currás, D. Kang, F. Ricci, K. W. Plaxco, *J. Am. Chem. Soc.* **2016**, *138*, 15809–15812; b) H. Li, S. Li, J. Dai, C. Li, M. Zhu, H. Li, X. Lou, F. Xia, K. W. Plaxco, *Chem. Sci.* **2019**, *10*, 10843–10848; c) S. Li, A. Ferrer-Ruiz, J. Dai, J. Ramos-Soriano, X. Du, M. Zhu, W. Zhang, Y. Wang, M. Á. Herranz, L. Jing, Z. Zhang, H. Li, F. Xia, N. Martín, *Chem. Sci.* **2022**, *13*, 8813–8820.
[15] M. A. Pellitero, N. Kundu, J. Sczepanski, N. Arroyo-Currás, *Analyst* **2023**, *148*, 806–813.
[16] J. D. Mahlum, M. A. Pellitero, N. Arroyo-Currás, *J. Phys. Chem. C* **2021**, *125*, 9038–9049.
[17] a) A. Shaver, N. Kundu, B. E. Young, P. A. Vieira, J. T. Sczepanski, N. Arroyo-Currás, *Langmuir* **2021**, *37*, 5213–5221; b) S. Slavkovic, Z. R. Churcher, P. E. Johnson, *Bioorg. Med. Chem.* **2018**, *26*, 5427–5434; c) R. J. White, A. A. Rowe, K. W. Plaxco, *Analyst* **2010**, *135*, 589–594; d) E. Rahbarimehr, H. P. Chao, Z. R. Churcher, S. Slavkovic, Y. A. Kaiyum, P. E. Johnson, P. Dauphin-Ducharme, *Anal. Chem.* **2023**, *95*, 2229–2237.
[18] M. N. Stojanovic, P. de Prada, D. W. Landry, *J. Am. Chem. Soc.* **2000**, *122*, 11547–11548.
[19] M. Lovrić, Š. Komorsky-Lovric, *J. Electroanal. Chem. Interfacial Electrochem.* **1988**, *248*, 239–253.
[20] a) P. Newton, A. Simpson, S. Wanwimolruk, P. Maliakal, L. Villegas, D. Kuypers, N. J. White, *Eur. J. Clin. Pharmacol.* **2001**, *57*, 111–113; b) F. Kloprogge, V. Jullien, P. Piola, M. Dhorda, S. Muwanga, F. Nosten, N. P. J. Day, N. J. White, P. J. Guerin, J. Tarning, *J. Antimicrob. Chemother.* **2014**, *69*, 3033–3040.
[21] a) R. Rohs, H. Sklenar, R. Lavery, B. Röder, *J. Am. Chem. Soc.* **2000**, *122*, 2860–2866; b) E. Tuite, B. Norden, *J. Am. Chem. Soc.* **1994**, *116*, 7548–7556.
[22] Y. Biniuri, G.-F. Luo, M. Fadeev, V. Wulf, I. Willner, *J. Am. Chem. Soc.* **2019**, *141*, 15567–15576.
[23] M. A. D. Neves, S. Slavkovic, Z. R. Churcher, P. E. Johnson, *Nucleic Acids Res.* **2017**, *45*, 1041–1048.
[24] P. O. Vardevanyan, A. P. Antonyan, M. A. Parsadanyan, M. A. Shahinyan, L. A. Hambardzumyan, *J. Appl. Spectrosc.* **2013**, *80*, 595–599.
[25] a) O. Reinstein, M. Yoo, C. Han, T. Palmo, S. A. Beckham, M. C. J. Wilce, P. E. Johnson, *Biochemistry* **2013**, *52*, 8652–8662; b) Z. R. Churcher, D. Garaev, H. N. Hunter, P. E. Johnson, *Biophys. J.* **2020**, *119*, 1147–1156; c) Z. R. Churcher, M. A. D. Neves, H. N. Hunter, P. E. Johnson, *J. Biomol. NMR* **2017**, *68*, 33–39; d) M. A. D. Neves, A. A. Shoara, O. Reinstein, O. Abbasi Borhani, T. R. Martin, P. E. Johnson, *ACS Sens.* **2017**, *2*, 1539–1545.
[26] a) A. J. Van Riesen, J. Le, S. Slavkovic, Z. R. Churcher, A. A. Shoara, P. E. Johnson, R. A. Manderville, *ACS Appl. Bio Mater.* **2021**, *4*, 6732–6741; b) A. J. Van Riesen, B. Kalnitsky, A. A. Shoara, S. Slavkovic, Z. R. Churcher, P. E. Johnson, R. A. Manderville, *Dyes Pigm.* **2023**, *209*, 110936.
[27] a) M. Kurnik, G. Ortega, P. Dauphin-Ducharme, H. Li, A. Caceres, K. W. Plaxco, *Proc. Natl. Acad. Sci. USA* **2018**, *115*, 8352–8357; b) A. Idili, F. Ricci, A. Vallée-Bélisle, *Nucleic Acids Res.* **2017**, *45*, 7571–7580; c) G. Ortega, M. Kurnik, P. Dauphin-Ducharme, H. Li, N. Arroyo-Currás, A. Caceres, K. W. Plaxco, *Angew. Chem.* **2019**, *131*, 1728–1732; *Angew. Chem. Int. Ed.* **2019**, *58*, 1714–1718.
[28] A. A. Shoara, S. Slavkovic, L. W. Donaldson, P. E. Johnson, *Can. J. Chem.* **2017**, *95*, 1253–1260.
[29] M. A. D. Neves, O. Reinstein, M. Saad, P. E. Johnson, *Biophys. Chem.* **2010**, *153*, 9–16.
[30] L. Kékedy-Nagy, S. Shipovskov, E. E. Ferapontova, *Anal. Chem.* **2016**, *88*, 7984–7990.
[31] A. Martin, L. Bouffier, K. B. Grant, B. Limoges, D. Marchal, *Analyst* **2016**, *141*, 4196–4203.
[32] a) P. Dauphin-Ducharme, K. L. Ploense, N. Arroyo-Currás, T. E. Kippin, K. W. Plaxco, in *Biomedical Engineering Technologies: Volume 1* (Eds.: M. R. Ossandon, H. Baker, A. Rasooly), Springer US, New York, NY, **2022**, pp. 479–492; b) Y. Xiao, R. Y. Lai, K. W. Plaxco, *Nat. Protoc.* **2007**, *2*, 2875–2880.
[33] A. M. Downs, J. Gerson, K. L. Ploense, K. W. Plaxco, P. Dauphin-Ducharme, *Anal. Chem.* **2020**, *92*, 14063–14068.
[34] a) S. Slavkovic, P. E. Johnson, *Aptamers* **2018**, *2*, 45–51; b) S. Slavkovic, P. E. Johnson, in *Nucleic Acid Aptamers: Selection, Characterization, and Application* (Eds.: G. Mayer, M. M. Menger), Springer US, New York, NY, **2023**, pp. 105–118.
[35] A. A. Shoara, P. E. Johnson, *Aptamers* **2022**, *6*, 19–27.
[36] Z. R. Churcher, P. E. Johnson, *Aptamers* **2020**, *4*, 3–9.

Manuscript received: February 24, 2023
Accepted manuscript online: March 29, 2023
Version of record online: ■■, ■■

RESEARCH ARTICLE

Electrochemical aptamer-based (E-AB) biosensors: Here we show that methylene blue-modified E-AB sensors designed with the cocaine-binding aptamer, in contrast to the widely accepted binding-induced conformational change mechanism, rather undergoes a "redox reporter-ligand competition" mechanism. We foresee that our proposed mechanism will open new avenues in designing aptamers and E-AB sensors.

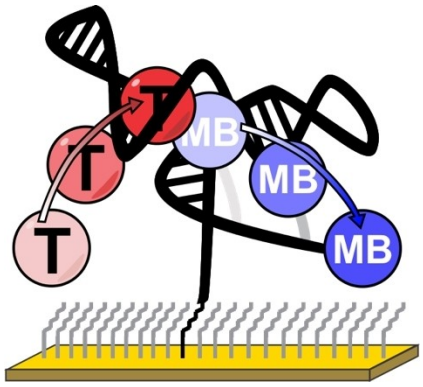

Dr. P. Dauphin-Ducharme, Dr. Z. R. Churcher, Dr. A. A. Shoara, E. Rahbarimehr, Dr. S. Slavkovic, Dr. N. Fontaine, O. Boisvert, Dr. P. E. Johnson**

1 – 10

Redox Reporter - Ligand Competition to Support Signaling in the Cocaine-Binding Electrochemical Aptamer-Based Biosensor